

# Drawing of virgin ultrahigh molecular weight polyethylene: an alternative route to high strength/high modulus materials

## Part 2 *Influence of polymerization temperature*

PAUL SMITH\*, HENRI D. CHANZY†, BRUNO P. ROTZINGER§

*E. I. du Pont de Nemours and Company, Inc., Central Research and Development Department, Experimental Station, Wilmington, Delaware 19898, USA*

The synthesis of ultra-high molecular weight polyethylene films and the production of high strength/high modulus tapes and filaments drawn directly from the virgin polymer are described. The study particularly focuses on the effect of the polymerization temperature on the deformation behaviour of the virgin UHMW polyethylene films. These results are discussed within the framework of the entanglement concepts for deformation of weakly bonded macromolecules. The development of the room temperature Young's modulus and the tensile strength with draw ratio is presented and compared with modulus and tenacity/draw ratio relations observed for melt and solution crystallized polyethylene.

### 1. Introduction

The structure and morphology of virgin, i.e. as-polymerized or nascent, crystallizable polymers has been a topic of interest in the 1960s [1-5]. In these early studies it was already recognized that under certain experimental conditions monomers may simultaneously polymerize and crystallize into chain-extended structures. The mechanism underlying this interesting polymerization is reasonably well understood [1-5]. Macromolecules polymerized below their melting point, or, rather, dissolution temperature in the polymerization mixture, never experience the liberty of the completely liquid state; only a part of the growing molecule is "dissolved" in its surrounding medium. The macromolecules thus never adopt a random coil conformation and, important in relation to the present work, do not form many entanglements with neighbouring chains. The actual temperature, pressure and concentration determine how many segments of the growing chain are in the liquid state; that is true if the polymerization rate does not exceed the rate at which the polymer segments are incorporated into the crystalline solid (schematically illustrated in Fig. 1 for Ziegler-Natta type ethylene polymerization). Thus it can readily be envisaged that under selected experimental conditions virgin polymers are produced in which the macromolecules exhibit a chain-extended and virtually "non-entangled" conformation. An example of a polymer produced commercially under such experimental conditions is poly(tetrafluoroethylene) (PTFE) [6-8]. As a result, virgin PTFE has a number of properties that are

remarkable in comparison with those of the once-molten (and re-entangled) polymer: a very high crystallinity, high melting temperature [9] and most unusual flow characteristics of the solid polymer [10].

In Part 1 [11] we described preliminary results on drawing of virgin ultra-high molecular weight (UHMW) polyethylene as an alternative route to high strength fibres. The presented method dispenses with the elaborate dissolution, precipitation and solvent recovery procedures in the "gel-spinning" technique [12, 13] that are necessary to untangle the long macromolecules prior to tensile drawing [14]. The alternative virgin-polymer processing technique [11] relies on the synthesis of polyethylene under experimental conditions where the macromolecules are produced in a near non-entangled conformation.

In view of the foregoing introductory remarks on virgin polymers, it is evident that the polymerization variables, such as temperature and pressure have a major effect on the conformation of the macromolecules produced and, therefore, on the properties of the as-polymerized polymer. In this paper we report on the effect of the polymerization temperature on the drawing characteristics of virgin UHMW polyethylene.

### 2. Experimental techniques

Virgin polyethylene films were produced according to the technique that was previously described [11, 15, 16]. A rack containing six cleaned glass slides was immersed in a boiling solution of 1 mM freshly distilled  $VCl_4$  in dry *n*-heptane. After 10 min a coating of fine  $VCl_3$

\* Present address: University of California, Materials Program, Santa Barbara, California 93106, USA.

† Permanent address: CERMAV (CNRS), BP 68, 38402 Saint Martin d'Herès, France.

§ Present address: Ciba-Geigy AG, Zentrales Forschungslaboratorium, CH-4002 Basel, Switzerland.

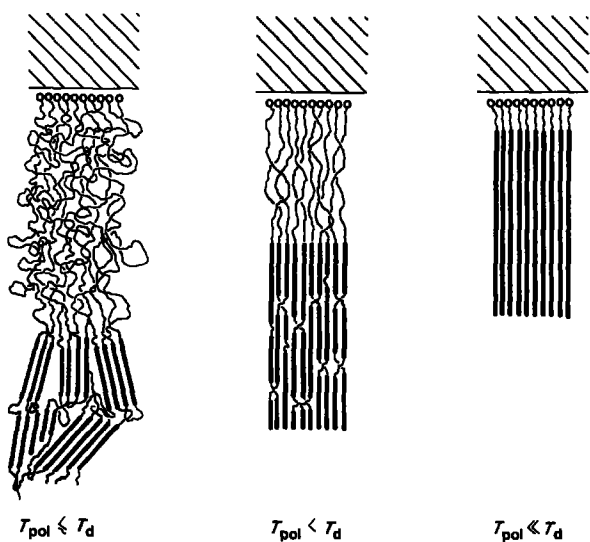


Figure 1 Schematic representation of the presumed effect of the polymerization temperature,  $T_{pol}$ , on the (partial) length of the growing macromolecule in the liquid state, and its effect on the resulting structure of the solid polymer.  $T_d$  is the dissolution temperature of a polymer molecule in the surrounding reaction medium. Shaded area represents Ziegler-Natta catalyst surface and (○) reaction sites.

crystals was deposited on to the slides. The glass slides were subsequently removed from the solution, washed with fresh heptane and inserted into a temperature-controlled polymerization reactor that was filled with a 3.6 mM solution of  $Al(CH_2CH(CH_3)_2)_3$ . Ethylene was bubbled through while the reaction mixture was stirred. The polymerization was performed at various (reactor) temperatures, ranging from  $-40$  to  $95^\circ C$ , and was continued for several hours. The resulting polyethylene-coated slides were removed from the reactor and washed with ethanol. The polymer films were readily stripped from the glass slides.

The inherent viscosity of the various polymer samples was measured in decalin at  $135^\circ C$ ; the polymer concentration was  $0.1\text{ g l}^{-1}$ . The inherent viscosities of all polyethylenes, independent of the polymerization temperature, was in the range 28 to  $30\text{ dl g}^{-1}$ , which corresponds to an average molecular weight ( $\bar{M}_v$ ) of  $\sim 4 \cdot 10^6$  [17].

Thermal properties of the polymer samples were examined by differential scanning calorimetry using a Mettler TA 3000 instrument. The sample weight was about 2 mg, and the scan speed was  $5^\circ C\text{ min}^{-1}$ . The melting points quoted in this paper invariably refer to the peak temperatures in the thermograms.

The drawing behaviour of the virgin polyethylene films was studied using an Instron Tensile Tester that was equipped with an environmental chamber. The tests were performed on dumb-bell-shaped specimens having a gauge length of 10 mm and a width of 0.5 mm. The testing speed was  $50\text{ mm min}^{-1}$  and the temperature was  $90^\circ C$ , unless indicated otherwise.

The morphology of the virgin as well as the drawn films was investigated by optical, and scanning and transmission electron microscopy using a Zeiss, Cambridge S 100 and Jeol 200 CX instrument, respectively. Wide-angle X-ray scattering studies were performed using a flat-film vacuum camera.

TABLE I Properties of virgin ultra-high molecular weight polyethylene films

$T$ (pol) ( $^\circ C$ )	$t$ (pol) (h)	Thickness ( $\mu\text{m}$ )	$T_m$ ( $^\circ C$ )	$\Delta H_f$ ( $\text{J g}^{-1}$ )	Crystallinity* (%)
-40	44	67	141.4	237	82
-10	16	73	140.0	234	81
20	6	40	139.5	231	80
50	5	55	138.7	206	71
95	4	13	139.1	215	74

\*100% =  $293\text{ J g}^{-1}$  [19].

### 3. Results and discussion

#### 3.1. Properties and structure of the virgin films

Some relevant characteristics of the virgin UHMW polyethylene (PE) films produced at various polymerization temperatures are presented in Table I. It should be noted the indicated polymerization temperatures refer, in fact, to the temperatures of the reaction vessel. The local temperature of the medium surrounding the polymerizing macromolecules is likely to be different. The thickness of most of the films was in the range from 40 to  $70\text{ }\mu\text{m}$ . Table I gives the polymer melting temperatures,  $T_m$ , and enthalpies of fusion,  $\Delta H_f$ , that were determined by differential scanning calorimetry (DSC). The values of  $T_m$  and  $\Delta H_f$  of the polyethylene samples were remarkably high, in accordance with previous findings [11, 16]; these values tended to increase with decreasing polymerization temperature. This result is, of course, in gratifying accord with the schematic illustration presented in Fig. 1.

Once molten and recrystallized, the polyethylene samples had a significantly lower melting temperature and heat of fusion. A typical set of DSC thermograms of virgin (polymerized at  $-40^\circ C$ ) and melt-recrystallized UHMW polyethylene is presented in Fig. 2. The melting temperature of all PE films that

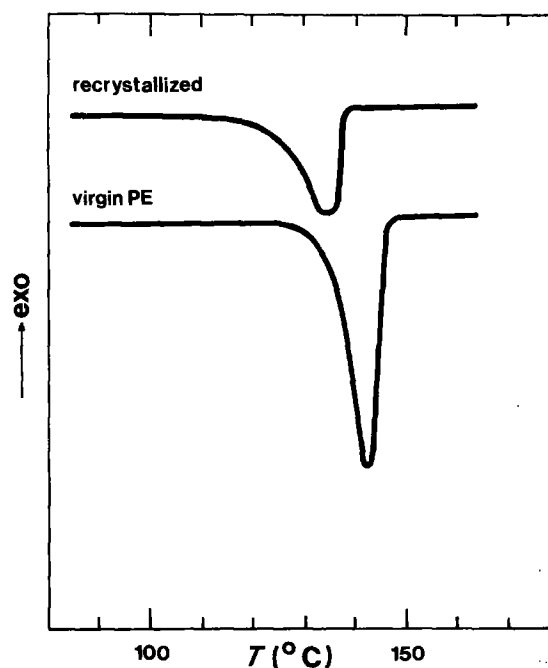


Figure 2 Differential scanning calorimetry curves of virgin and melt-recrystallized UHMW polyethylene ( $T_{pol} = -40^\circ C$ ; for details see Section 2). Scan speed  $5^\circ C\text{ min}^{-1}$ .

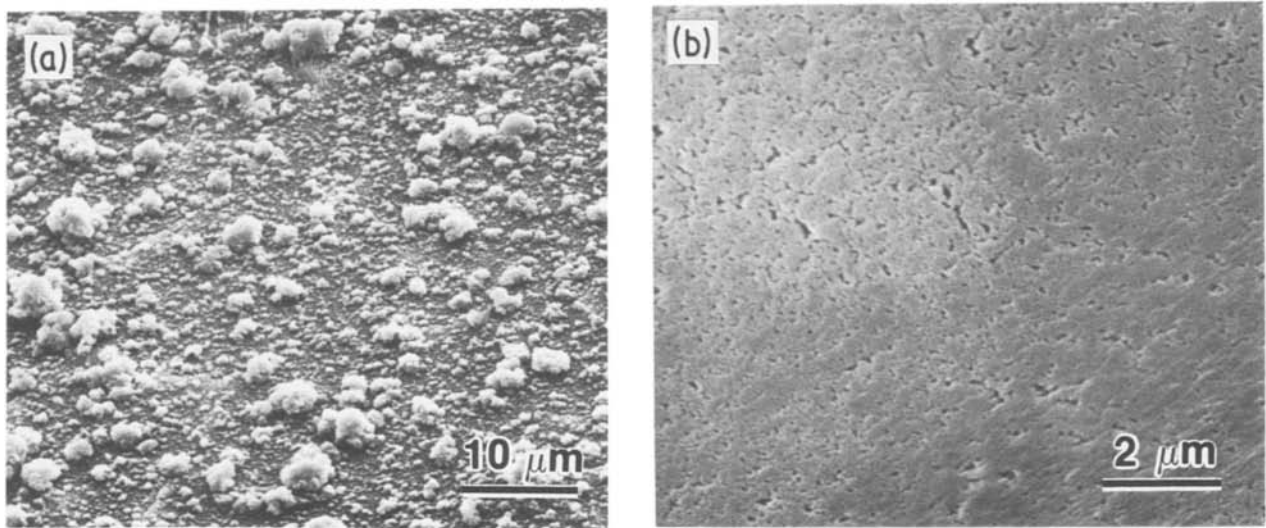


Figure 3 Typical scanning electron micrographs of (a) the (top) surface and (b) bottom (glass-side) of virgin UHMW polyethylene films.

were recrystallized from the melt was  $\sim 133^\circ\text{C}$  and their heat of fusion was about  $130\text{ J g}^{-1}$  ( $\sim 45\%$  crystallinity) (see also [18]). Such large differences between the values of  $T_m$  and  $\Delta H_f$  of virgin and once-molten polymer has been reported for many other polymers, notably for poly(tetrafluoroethylene) (e.g. [10]).

The morphology and structure of the virgin films was investigated by scanning electron microscopy (SEM) and wide-angle X-ray scattering (WAXS). It was discussed in Part 1 [11] that the virgin PE films had a smooth bottom (glass-side) surface and a somewhat irregular top (see Fig. 3). The inner structure of the PE films was revealed by fracturing the specimens

in liquid nitrogen. Figs 4a, b and c show scanning electron micrographs of fracture surfaces of the films polymerized at, respectively,  $-40$ ,  $50$  and  $95^\circ\text{C}$ . The film polymerized at the lowest temperature ( $-40^\circ\text{C}$ , Fig. 4a) appeared to be characterized by a relatively smooth fracture surface. The photograph in Fig. 4a shows some preferred orientation normal to the film plane. This will be substantiated and elaborated upon below (Fig. 5). At progressively higher polymerization temperatures (Figs 4b and c) the virgin PE films displayed an increasingly rough fracture surface morphology which points, in our view, to an increasing intermolecular coherence, i.e. enhanced chain entanglement.

Fig. 5a shows a high-resolution scanning electron micrograph of a fracture surface of the virgin PE film produced at  $-40^\circ\text{C}$ . This photograph reveals a striated or fibrillar texture oriented perpendicular to the film surface (refer to sketch Fig. 5b). A wide-angle X-ray pattern taken in the direction of the film plane is displayed in Fig. 5c. This WAXS pattern indicates a relatively poor, but noticeable  $c$ -axis orientation of the polyethylene chains normal to the film surface.

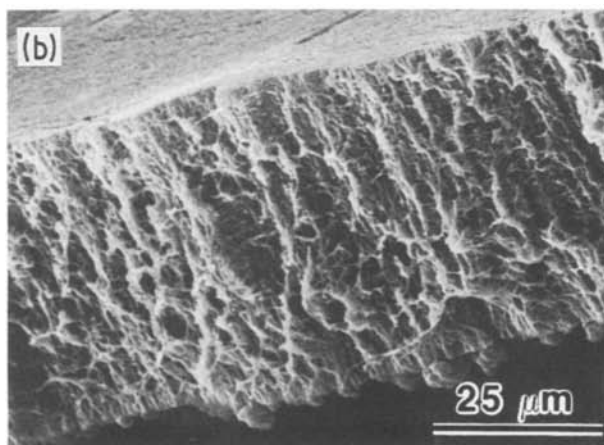
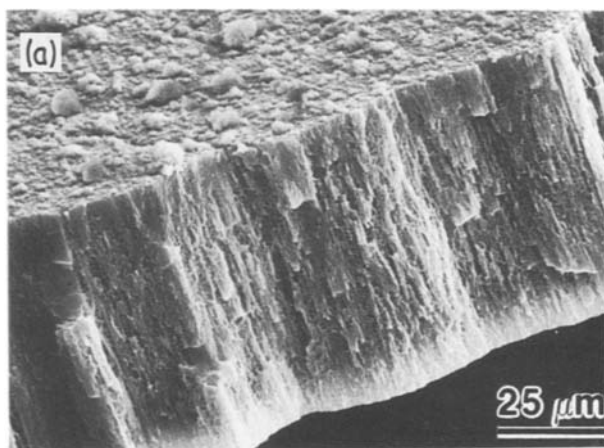
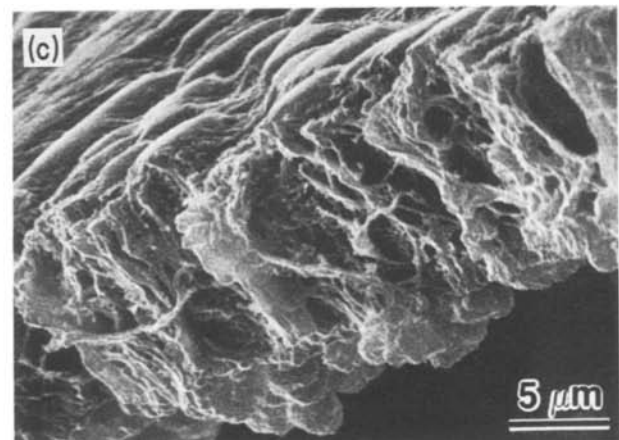
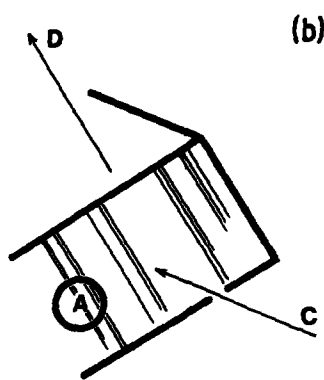
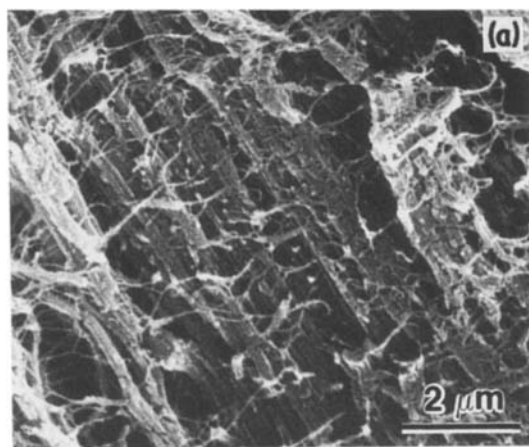
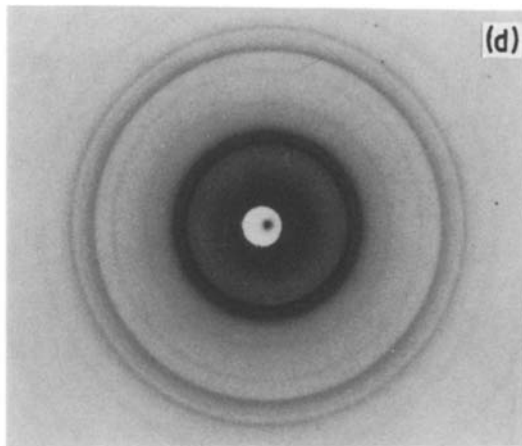
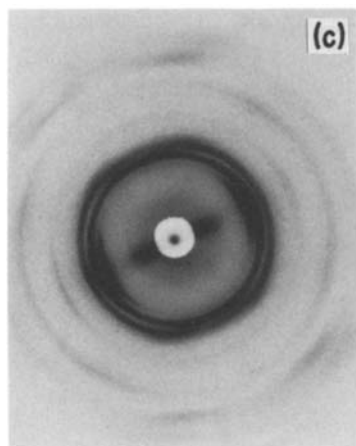


Figure 4 Scanning electron micrographs of fracture surfaces, produced in liquid nitrogen, of virgin UHMW PE films polymerized at (a)  $-40^\circ\text{C}$ , (b)  $50^\circ\text{C}$  and (c)  $95^\circ\text{C}$ . Note the increased roughness of the fracture surface at increasing polymerization temperature.





**Figure 5** (a) Scanning electron micrograph of a fracture surface (in liquid nitrogen) of the virgin PE film that was polymerized at  $-40^{\circ}\text{C}$ . This micrograph reveals the fibrillar structure oriented normal to the film surface. (b) Schematic illustration of the orientation of (a) and (c, d) wide-angle X-ray scattering patterns with respect to the virgin PE film. (c) WAXS-pattern taken parallel to the film surface. This pattern is indicative of *c*-axis orientation normal to the plane of the virgin PE film. (d) WAXS through-pattern. Note the occurrence in the patterns (c) and (d) of additional reflections due to the presence of the triclinic polyethylene crystal modification.



This in contrast with earlier findings on the structure of nascent polyethylene films [15]. The latter films were polymerized, however, at higher temperatures, which expectedly (see Fig. 1) has an adverse effect on *c*-axis orientation. Indeed, in the present study it was found that the *c*-axis orientation normal to the film surface rapidly deteriorated at increasing temperatures. For a more complete description of the structure and morphology of virgin polyethylene films polymerized at elevated temperatures the reader is referred to Chanzy *et al.* [15]. Fig. 5d, finally, shows a WAXS-pattern taken normal to the plane of the film. The diffractograms in Figs 5c and d show the presence of a marked fraction of the triclinic [20] crystal modification, besides the usual orthorhombic crystal structure of polyethylene. The occurrence of the triclinic phase in virgin polyethylene has been reported previously [15], and it was interpreted as indicative of substantial stresses arising during insertion of the monomer into the catalyst-polymer bond. Inspection of the WAXS pattern in Fig. 5c reveals that it is primarily this triclinic phase that appeared to display a preferred orientation, which seems to substantiate this mechanism.

The amount of the triclinic crystalline phase was found to decrease at increasing polymerization temperature. Fig. 6 shows  $2\theta$  X-ray scans recorded normal to the film plane of virgin PE polymerized at  $-40$ ,  $25$  and  $95^{\circ}\text{C}$ , illustrating the disappearance of the additional (010) and (100) triclinic unit cell reflections at increasing polymerization temperatures.

### 3.2. Deformation behaviour

The virgin polyethylene films displayed remarkable differences in their deformation behaviour. The scanning electron micrographs of Figs 7a, b and c show the very different morphologies resulting from deformation at room temperature of the PE films polymerized at  $-40$ ,  $50$  and  $95^{\circ}\text{C}$ , respectively. Fig. 7a shows that the films polymerized at  $-40^{\circ}\text{C}$  could not be drawn but failed in a ductile mode. Close inspection of the fracture surface revealed numerous fibrils that were pulled out from the undeformed material. These fibrils apparently were incapable of sustaining or transmitting the drawing force. The film produced at  $-10^{\circ}\text{C}$  displayed a similar behaviour. An optical micrograph of the PE film polymerized at  $50^{\circ}\text{C}$ , and subsequently drawn at room temperature, is presented in Fig. 7b. This picture shows the familiar "neck" formation. Upon further drawing more and more unoriented material was transformed into highly oriented fibrils, until the entire specimen was "drawn". Fig. 7c of the PE film polymerized at  $95^{\circ}\text{C}$  displays yet another response to room-temperature drawing. This particular film appeared to deform in a macroscopically homogeneous fashion, i.e. without the formation of a visible neck. The scanning electron micrograph of Fig. 7c shows, however, that the deformation was by no means homogeneous on a smaller scale ( $\sim 10\ \mu\text{m}$ ) and had resulted in the formation of a great many micro-necks.

This transformation from ductile failure to necking and to multiple micro-necking, reported here for

virgin UHMW PE films produced at different polymerization temperatures, was previously observed for dried gel films of UHMW polyethylene that were cast from solutions of different initial polymer concentration (for details see [21]).

The differences in drawing characteristics of the virgin PE films polymerized at different temperatures were unveiled more quantitatively in tensile tests. Fig. 8 shows a set of nominal stress/strain curves recorded at 90°C of the various virgin polyethylene films. The temperatures in this figure indicate the polymerization temperature. The relatively low testing temperature of 90°C was selected in order to prevent thermally induced changes of the original polymer films, such as excessive annealing or even partial melting. Fig. 8 shows that all the PE films, independent of the polymerization temperature, exhibited a yield stress (at 90°C) of about 3 MPa. This important finding indicates that the small strain coherence of the films was comparable. The post-yield behaviour, was, however, dramatically different for the various films. Films polymerized at -40, -10 and 20°C all displayed a negative slope of the stress/strain curve after the yield point, i.e. strain softening. As a result, these films could not be homogeneously drawn to high elongations. The stress/strain curve of the sample produced at 50°C was characterized by a nearly constant (nominal) drawing stress, and the high draw ratio of 46 was obtained at the relatively low drawing temperature of 90°C. Such a constant nominal stress/strain curve was earlier identified as optimal for the production of high modulus materials [14]. Finally, the slope of the nominal stress/strain curve of the film

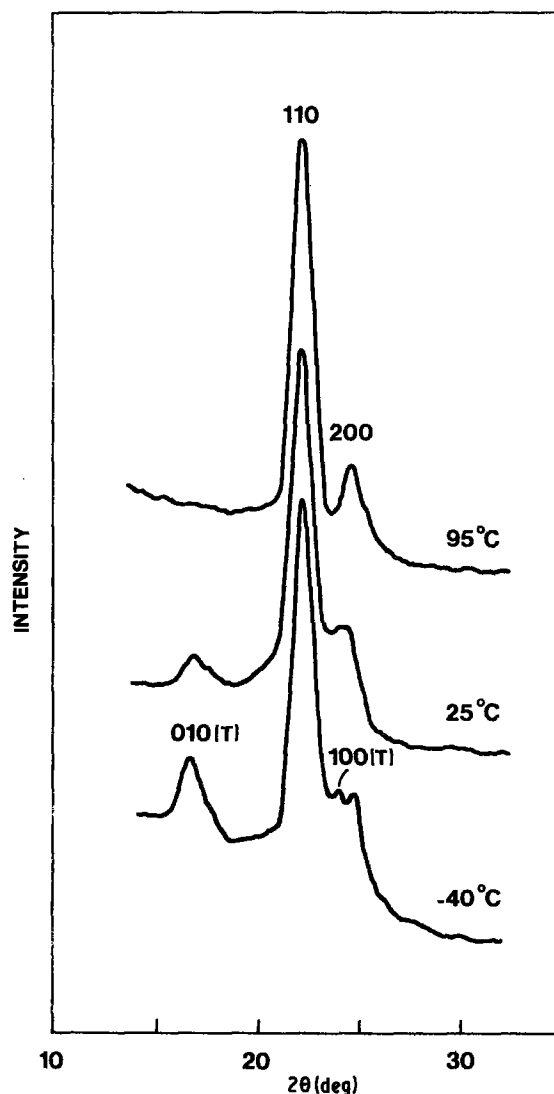


Figure 6  $2\theta$  X-ray scans recorded normal to the surface of virgin PE films that were polymerized at different temperatures (indicated in graph). Note the gradual disappearance with increasing polymerization temperatures of the (010) and (100) reflections associated with the triclinic unit cell.

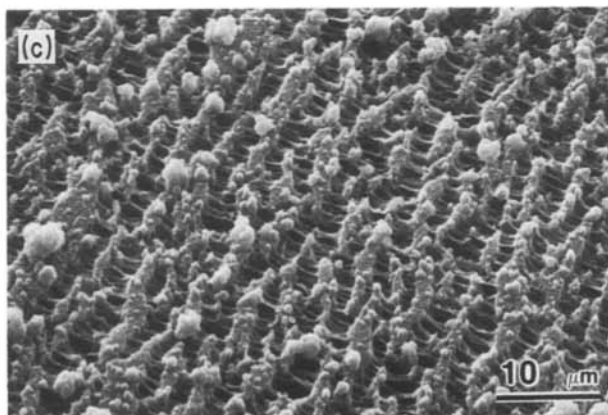
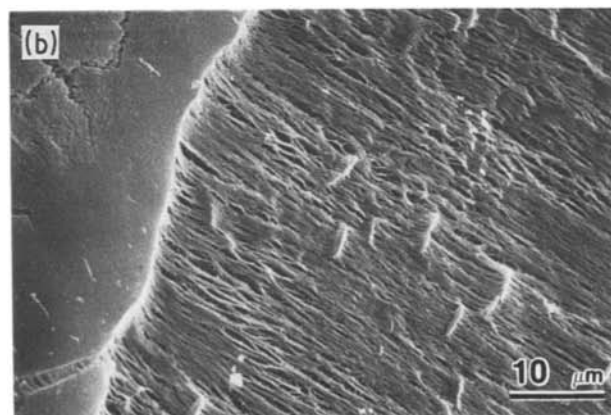
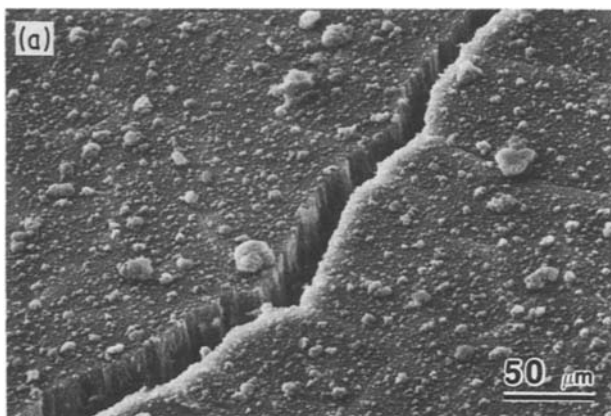


Figure 7 Scanning electron micrographs of various virgin UHMW polyethylene films drawn at room temperature. Polymerization temperatures: (a) -40°C, (b) 50°C and (c) 95°C. Note the transition from ductile fracture (a) to necking (b) and to micro-necking (c) at increasing polymerization temperature.

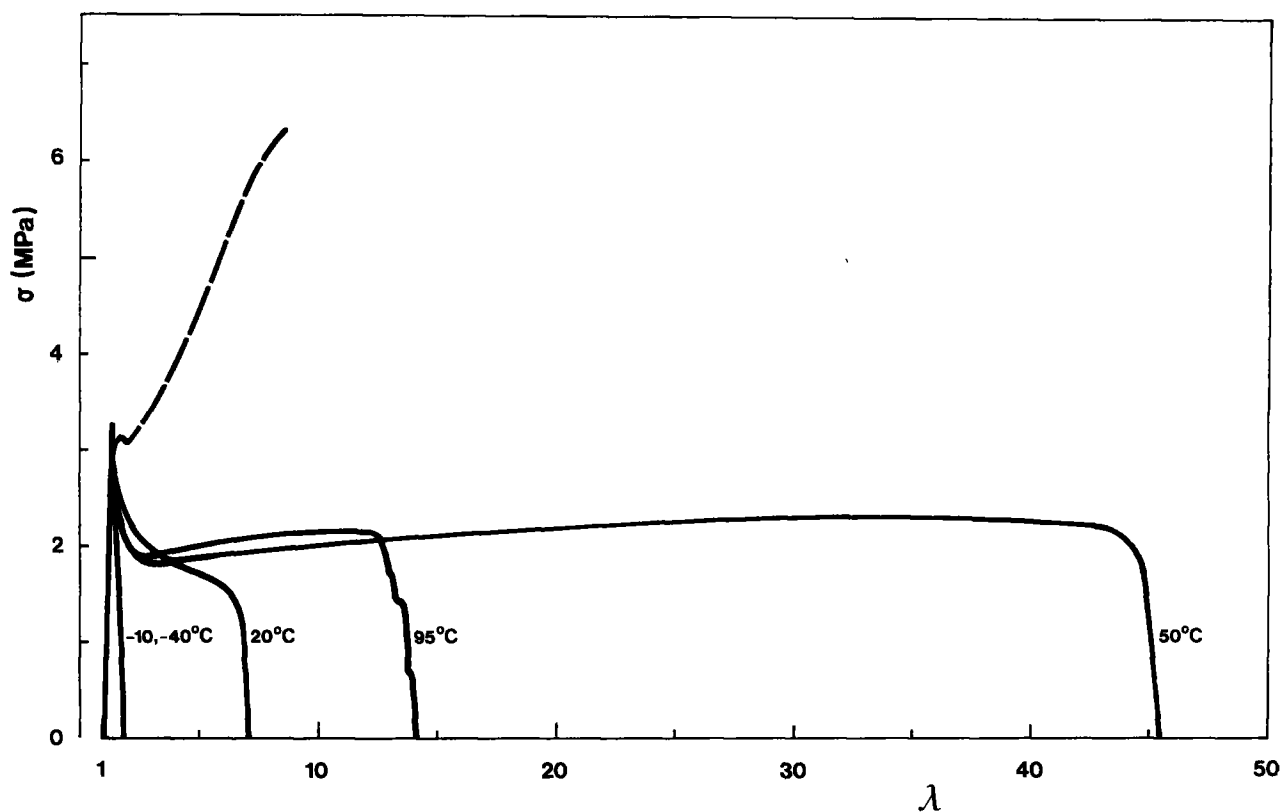


Figure 8 Nominal stress-strain curves, recorded at  $90^{\circ}\text{C}$  and  $25\text{ mm min}^{-1}$  ( $L_0 = 10\text{ mm}$ ), of virgin UHMW polyethylene films polymerized at various temperatures (indicated in graph). Also represented is a typical stress-strain curve of melt-recrystallized films (broken curve).

polymerized at  $95^{\circ}\text{C}$  was slightly positive; the maximum draw ratio was only 16.

The systematic increase of the nominal post-yield stress with strain, observed here at increasing polymerization temperature, was previously reported to occur with increasing initial polymer concentration of solution cast gel films of UHMW PE [14]. The latter result was attributed to increased entanglement densities in solids that were precipitated from increasingly concentrated solutions. In fact, the systematic dependence on the initial polymer concentration of the post-yield behaviour and the maximum draw ratio of solution-cast, or -spun, gel films was interpreted as experimental proof for the concept that the deformation of polyethylene is dominated by trapped entanglements [14]. Within that context the presently observed differences in the deformation behaviour of the UHMW polyethylene films, produced at different temperatures, indicate that the entanglement density in the virgin films is systematically dependent on the polymerization temperature, which is in accordance with the hypothesis discussed in Section 1.

The differences in drawing behaviour of the films polymerized at various temperatures were completely lost upon melting and recrystallization. Fig. 8 displays a typical stress/strain curve, recorded at  $90^{\circ}\text{C}$ , of once-molten and recrystallized PE films. The maximum draw ratio of these melt-recrystallized films was about 8. This result can, of course, readily be explained in terms of reentangling upon melting.

### 3.3. Properties of drawn films

Strips (initial width about  $0.5\text{ mm}$ , length  $10\text{ mm}$ ) of the film polymerized at  $50^{\circ}\text{C}$  were drawn to various

draw ratios at  $120^{\circ}\text{C}$  and at a rate of elongation of  $50\text{ mm min}^{-1}$ . The mechanical properties of these drawn ribbon-shaped filaments were measured at room temperature. The gauge length was  $25\text{ mm}$  and the testing speed was  $25\text{ mm min}^{-1}$ .

Fig. 9a shows the initial (Young's) modulus plotted against draw ratio of the virgin polyethylene filaments. The broken curve in this figure represents the modulus/draw ratio relationship for both melt- [22] and solution-spun [12, 23] polyethylene samples drawn under the most efficient drawing conditions. Previously, it was demonstrated that this modulus/draw ratio relationship was well-described with a zero-parameter model based on affine deformation of randomly coiled macromolecules [24]. Fig. 9 shows that deformation of the virgin polyethylene films resulted in a more rapid increase of the modulus with draw ratio than for melt or solution processed polyethylene. For example, the present virgin UHMW PE films have a Young's modulus of  $65\text{ MPa}$  at a draw ratio of 20, compared to a value of 40 to  $45\text{ GPa}$  for optimally drawn melt or solution crystallized polyethylene [12, 22, 23]. This observation can readily be explained by a non-random coil, or pre-extended, conformation of the polyethylene macromolecules in the undrawn virgin polymer. This is, in fact, very likely in view of the mechanism of polymerization described in Section 1.

Fig. 9b shows a plot of the tensile stress at break against the draw ratio. Typical cross-sectional dimensions of the drawn filaments were  $2\text{ to }4 \times 10^{-4}\text{ mm}^2$  ( $\sim 2\text{ to }4\text{ denier}$ ). This graph illustrates that the virgin polyethylene produced in this study can readily be drawn into filaments having a tenacity of more than

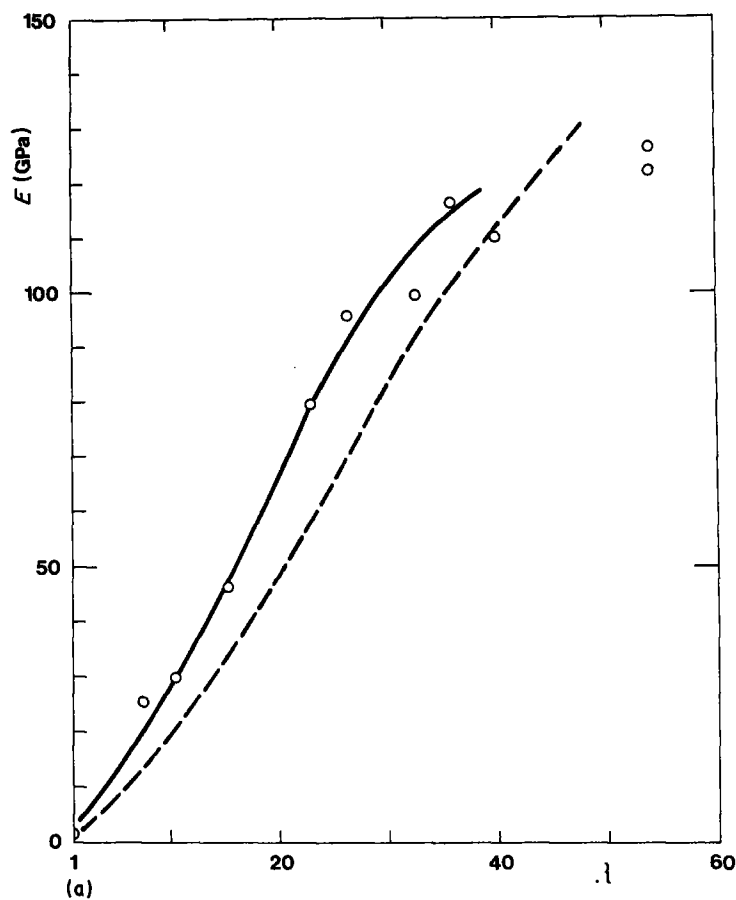
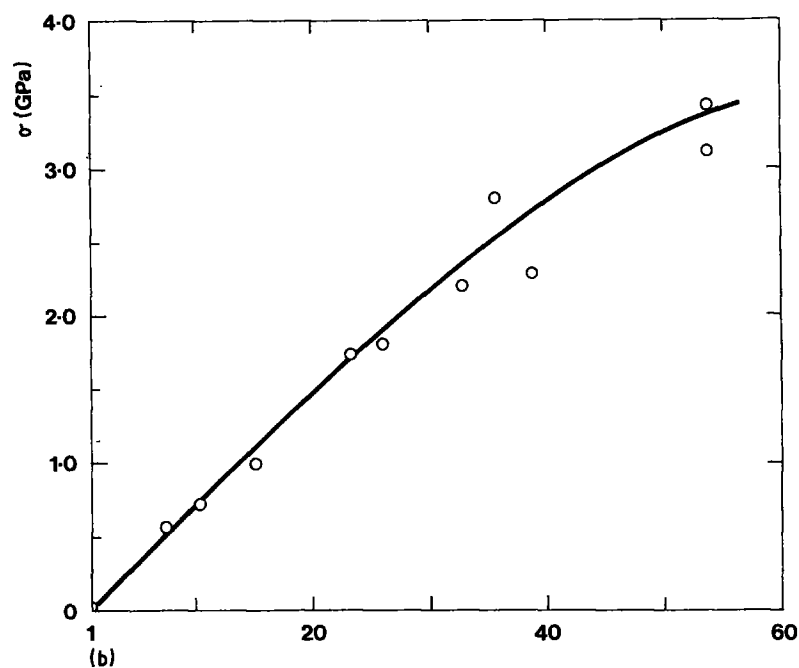


Figure 9 (a) Room temperature Young's modulus plotted against draw ratio of virgin UHMW PE films polymerized at 50° C. Drawing temperature 130° C. Broken line represents the modulus/draw ratio relation for affinely deformed melt or solution crystallized polyethylene (see text). (b) Corresponding plot of the room temperature tensile strength plotted against draw ratio. Cross-sectional area of the drawn, tape-shaped, filaments was 2 to 4 × 10<sup>-4</sup> mm<sup>2</sup> (~2 to 4 denier).



3 GPa. The values of the tenacity appear to be slightly below (~15%) those of solution-spun (commonly known as "gel"-spun) filaments of similar molecular weight [12, 13, 23] at identical modulus. It is thought that this small reduction in tensile strength is due to some defects resulting from inhomogeneous catalyst deposition (cf. Fig. 11 below).

The elongation at break of the drawn virgin PE filaments was found in the range from 3.5 to 4.5%.

### 3.4. Morphology and structure

In this section we briefly describe some morphological

features of the highly drawn virgin polyethylene filaments.

Fig. 10 displays a high-resolution scanning electron micrograph of a 60 times drawn ribbon-shaped filament. The micrograph shows the "bottom" side, i.e. the side that faced the glass slide in the original virgin film (cf. Fig. 3b). This surface of the ribbon appeared to be essentially defect free and of a fibrillar texture, as is commonly found for such highly drawn materials. Fig. 11 shows a lower magnification electron micrograph of the "top" side of the same ribbon. This picture reveals the presence of particle-like defects on

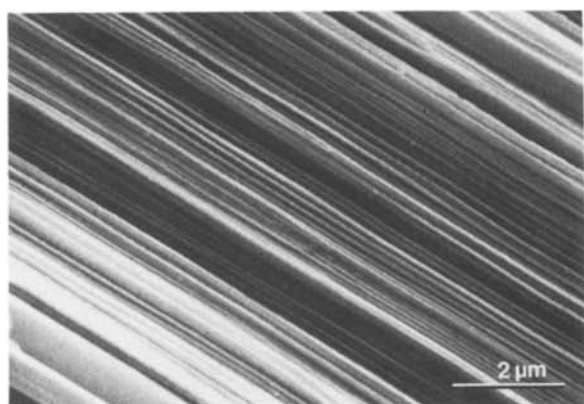


**Figure 10** Scanning electron micrograph of 60 times drawn virgin UHMW PE tape-shaped filament. This micrograph was taken of the “bottom” side, that faced the glass slide in the original, undrawn film.

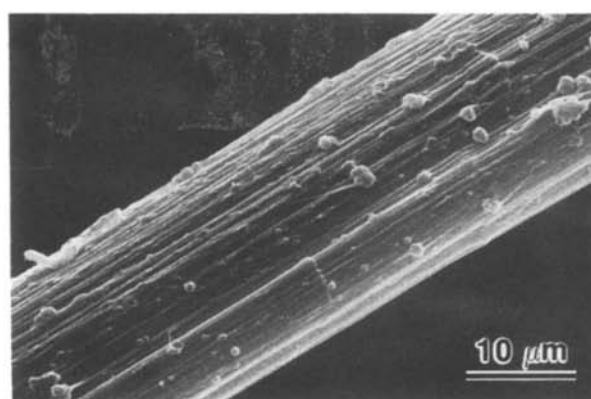


**Figure 11** Scanning electron micrograph of highly drawn strip of virgin UHMW PE film. This photomicrograph, which was taken of the “top” side (cf. Fig. 3a), reveals remaining particle-like defects on the filament surface.

the surface of the filament. These defects, which are thought to originate in inhomogeneous catalyst deposition, are likely to be responsible for the slightly lower tenacity of the present drawn virgin PE filaments in comparison with the gel-spun fibres, as was mentioned above.

Fig. 12, finally, shows two typical electron diffraction through-patterns of a 60 times drawn virgin UHMW PE film. The patterns indicate a double orientation in the highly drawn tapes. The *c*-axis appears perfectly lined up into the direction of draw (arrow) and the *a*-axis approximately normal to the film plane. Such double orientation was observed previously in solution-cast/drawn gel films of polyethylene [21, 25]. To the authors’ knowledge this orientation has not been found in drawn filaments having round cross-sections. It seems, therefore, likely that the double orientation is associated with factors dominated by the sample geometry; such as conditions of plane stress occurring in film drawing, which is unlike the stress distribution generally observed in deformation of fibres [26].

#### 4. Concluding remarks

In this paper we described the polymerization of ultra-high molecular weight polyethylene and the production of high performance films, tapes and fibres drawn directly, i.e. without additional processing, from the virgin polymer. The present process thus circumvents the laborious solution precipitation in the gel-spinning process – the crucial step required to disentangle the long macromolecules prior to (ultra)drawing. The present study particularly focused on the effect of the polymerization temperature on the deformation behaviour of the virgin polymer. We identified, for the present catalyst system, an “optimum” polymerization temperature (range) for the preparation of highly drawable UHMW PE films, suitable for the production of high strength/high modulus materials. Polymerizations carried out below the “optimal” temperature of about 50°C resulted in polyethylene films without sufficient intermolecular coherence; premature ductile fracture occurred during hot drawing of these as-polymerized films. Films produced at temperatures exceeding 50°C, on the other hand, exhibited

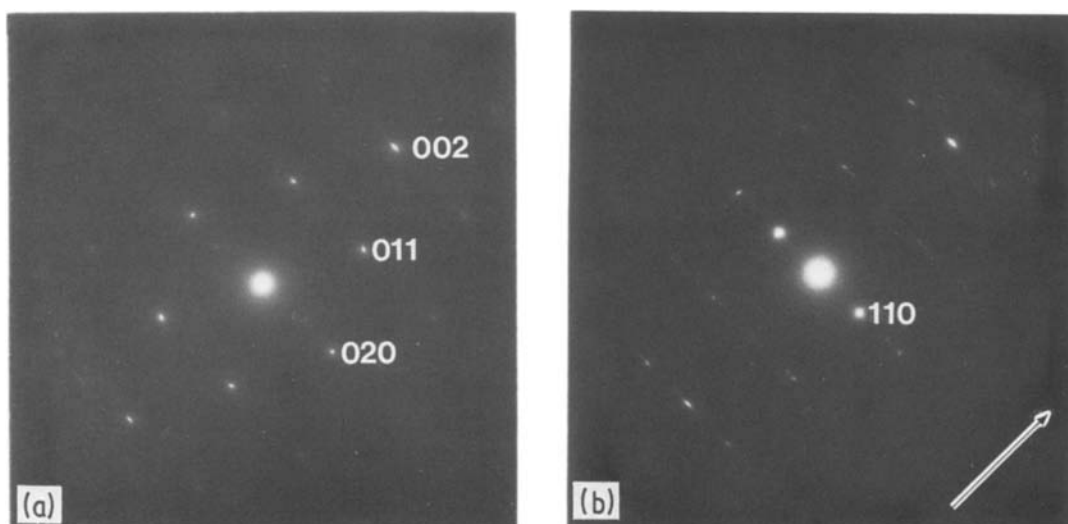


**Figure 12** Typical electron diffraction through-patterns of 60 times drawn virgin PE films. Arrow indicates draw direction. These patterns indicate a strong double orientation of the orthorhombic unit cell in the films, with the *c*- (molecular) axis lined up in the direction of draw and the *a*-axis approximately normal to the surface.



maximum draw ratios that were well below those achieved for films polymerized at this optimum temperature. These important differences in deformation behaviour of the various virgin PE films can be very well explained and readily understood in terms of a systematically decreasing entanglement density with decreasing polymerization temperature.

Caution should be exercised with the interpretation of the designation "optimum" polymerization temperature; it refers only to the polymerization and drawing conditions described in this paper. In general, the most favourable polymerization temperature will depend on the selection of the catalyst system, polymerization variables such as monomer pressure, etc. Moreover, it will depend on the particular conditions under which the samples are drawn, such as the strain rate and drawing temperature. Illustrative in this respect is, for example, the present finding that the UHMW PE film polymerized at room temperature could not be drawn to high draw ratios at a drawing temperature of 90°C (due to strain softening resulting from a lack of intermolecular coherence). When the deformation was performed, however, at 135°C this material could readily be drawn to the high draw ratio of 60×, as was reported in Part I [11]. Further study revealed that partial melting, associated with partial re-entangling, occurred upon annealing or processing the virgin polyethylene films above 120°C.

In addition to the particular conditions of drawing, post-polymerization treatments prior to drawing, such as annealing, partial melting, cold or hot pressing, solid-state pre-extrusion [27], etc., affect the performance of the various virgin PE films. These treatments are particularly of interest for processing the films prepared in this study at temperatures below 50°C, which were rejected here as "not-drawable" in the free-drawing experiment. Many of the techniques that have been developed for drawing of single crystal mats (e.g. [27–29]) can be employed to process these materials into high performance polyethylene. These topics, however, do not fall within the scope of the present study and will be addressed in more detail in a subsequent study.

### Acknowledgements

It is the authors' pleasure to acknowledge the skilled and efficient assistance of William R. Greene Jr. The authors also thank Margaret A. Ferrari for performing the X-ray measurements.

### References

1. B. WUNDERLICH, *Adv. Polym. Sci.* **5** (1968) 568.

2. R. H. MARCHESSAULT, B. FISA and H. D. CHANZY, *CRC Crit. Rev. Macromol. Sci.* October (1972) 315.
3. P. BLAIS and R. ST. JOHN MANLEY, *J. Polym. Sci. A-1* **6** (1968) 291.
4. A. KELLER and F. M. WILLMOUTH, *Makromol. Chem.* **121** (1969) 42.
5. B. WUNDERLICH, "Macromolecular Physics", Vol. 2 (Academic, New York, 1976) p. 189.
6. C. A. SPERATI and H. W. STARKWEATHER Jr, *Fortschr. Hochpolym.-Forsch.* **2** (1961) 465.
7. F. J. RAHL, M. A. EVANCO, R. J. FREDERICKS and A.-M. REIMSCHUESSEL, *J. Polym. Sci. A-2* **10** (1972) 1337.
8. H. D. CHANZY, P. SMITH and J.-F. REVOL, *J. Polym. Sci. Polym. Lett. Ed.* in press.
9. H. W. STARKWEATHER Jr, P. ZOLLER, G. A. JONES and A. J. VEGA, *J. Polym. Sci. Polym. Ed.* **20** (1982) 751.
10. H. W. STARKWEATHER Jr, *ibid.* **17** (1979) 73.
11. P. SMITH, H. D. CHANZY and B. P. ROTZINGER, *Polymer Commun.* **26** (1985) 258.
12. P. SMITH and P. J. LEMSTRA, *J. Mater. Sci.* **15** (1980) 505.
13. B. KALB and A. J. PENNING, *ibid.* **15** (1980) 2584.
14. P. SMITH, P. J. LEMSTRA and H. C. BOOIJ, *J. Polym. Sci. Polym. Phys. Ed.* **19** (1981) 877.
15. H. D. CHANZY, A. DAY and R. H. MARCHESSAULT, *Polymer* **8** (1967) 567.
16. R. H. MARCHESSAULT and H. D. CHANZY, *J. Polym. Sci. C* **30** (1970) 311.
17. H. L. WAGNER and J. G. DILLON, *ACS Polym. Mat. Sci. Eng.* **50** (1984) 53.
18. H. D. CHANZY, E. BONJOUR and R. H. MARCHESSAULT, *Colloid Polym. Sci.* **252** (1974) 8.
19. B. WUNDERLICH, "Macromolecular Physics", Vol. 3 (Academic, New York, 1980) p. 58.
20. P. W. TEARE and D. R. HOLMES, *J. Polym. Sci.* **24** (1957) 496.
21. P. SMITH, P. J. LEMSTRA, J. P. L. PIJPERS and A. M. KIEL, *Colloid Polym. Sci.* **259** (1981) 1070.
22. G. CAPACCIO, A. G. GIBSON and I. M. WARD, in "Ultra-High Modulus Polymers", edited by A. Ciferri, I. M. Ward (Applied Science, London, 1979) p. 12.
23. A. V. SAVITSKY, I. A. GORSHKOVA, I. L. FROLOVA, G. N. SHMIKK and A. F. IOFFE, *Polym. Bull.* **12** (1984) 195.
24. P. A. IRVINE and P. SMITH, *Macromolecules* **19** (1986) 240.
25. P. SMITH, A. BOUDET and H. D. CHANZY, *J. Mater. Sci.* **4** (1985) 13.
26. J. A. NAIRN, private communication.
27. T. KANAMOTO, A. TSURUTA, A. TANAKA and R. S. PORTER, *Polym. J.* **15** (1983) 327.
28. W. O. STATTON, *J. Appl. Phys.* **38** (1967) 4149.
29. M. MAEDA, K. MIYASAKA and K. ISHIKAWA, *J. Polym. Sci. A-2* **8** (1970) 355.
24. P. A. IRVINE and P. SMITH, *Macromolecules* **19** (1986) 240.

Received 13 March

and accepted 2 June 1986